



South Eastern Australian Climate initiative

Final report for Project 1.1.2

Comparing documented climate changes with those attributable to specific causes

Principal Investigator:

Dr. Bertrand Timbal

B.Timbal@bom.gov.au

Co-Authors:

**Dr Bradley Murphy, Dr Karl Braganza, Dr Harry Hendon, Dr Matt Wheeler and Mr
Clinton Rakich**

CSIRO Land and Water

Ph: 02 6246 5617

seaci@csiro.au

<http://www.seaci.org>



© 2010 CSIRO. To the extent permitted by law, all rights are reserved and no part of this publication covered by copyright may be reproduced or copied in any form or by any means except with the written permission of CSIRO.

Initial Project objectives

- To compare recent observed climate changes to variability associated with modes of climate features using up to date knowledge on the role of key large-scale modes of variability gathered as part of project 1.1.1
- Attribute the recent changes to possible external forcing with a focus on cold season rainfall decline in the south and warm season rainfall decline in the north and increased heat waves.

Proposed methodology

- Benefit from the review of the existing scientific literature on the climate of south-east Australia and the analysis of the importance of various large-scale modes of variability to focus on the most likely contributor to observed rainfall decline.
- Compare recent observed climate change to variability associated with the Southern Annular Mode (SAM) and evaluate the likelihood that the SAM has contributed to the observed rainfall decline directly or through the influence on local mean sea level pressure (MSLP).
- Investigate the causes of the changes of MSLP surrounding southern Australia and its role in relation to the rainfall decline in south-east Australia.
- Investigate the role of MSLP changes in explaining recent heat wave using as a case study the April 2005 Murray–Darling Basin wide heat wave.

Summary of the findings

- The autumn rainfall decline (60 per cent of the total rainfall decline) in south-eastern Australia (SEA) is a combination of autumn to early winter in the south and summer to autumn in the north. In the south, the decline started in the early 1990s but is only apparent since 2000 in the north. The two areas can be broadly separated by the location of the sub-tropical ridge (STR).
- In the south-western part of eastern Australia (SWEA), the Southern Annular Mode (SAM) has a negative impact on rainfall during a six-month period from May to October, which is when most of the total rainfall is encountered. In autumn as a whole, the SAM influence on rainfall in SEA is negligible, as the negative influence in May is cancelled out by the positive influence in summer extending to March. The modes of variability generated in tropical oceans (El Niño–Southern Oscillation – ENSO – and the Indian Ocean Dipole – IOD) are also unlikely to have contributed to the rainfall decline as if anything, their influence on the local rainfall is rather small and diminishing during the last the two decades.
- The SAM index has been trending upward. There is a positive trend in the 1980s and 1990s across summer and autumn but it does not translate into a rainfall decline.

Arguably, the trend extends to early winter (May to July) when the series is extended back in time to the 1960s and 1970s; this trend could have resulted in a rainfall decline of about 5 per cent in those decades, but did not.

- The SAM rainfall relationship is mostly felt through the local MSLP. The main control of MSLP over southern Australia is the intensity and location of the STR. The intensity of the STR has been trending upward since the 1970s and that can be translated into a sizeable rainfall decline (about 70 per cent of the observed decline in autumn to early winter: from March to July) using the correlation between the STR intensity and rainfall in SEA.
- The intensity of the STR also peaked in the 1940s at the time of the previous dry decade in south-eastern Australia. By and large during the 20th Century, the long-term evolution of the intensity of the STR follows the curve of the global temperature of the planet. This relationship gives a high likelihood that the current rainfall deficit is linked to the global warming of the planet, through the intensification of the STR.
- On the northern side of the STR, the rainfall relates well to a north-south MSLP gradient along the east coast (the Gayndah-Deniliquin Index or GDI). This index suggests a combination of long-term trends and decadal variability as the most likely explanation for the current rainfall deficit.
- Weather patterns do not explain the heat wave observed in April 2005, while the long term lower tropospheric warming trend appears as an important contribution. However, it does not appear to be the only explanation.

Technical details

Flow-on effects from project 1.1.1

The specifics of the rainfall decline across the south-east of Australia in the last 10 years were described in Murphy and Timbal (2007) as part of the Project 1.1.1. Key results emerging from this in-depth analysis is that although the rainfall decline is not unprecedented in the historical record, its consequences on the ground are, in particular in term of water resources. By comparing a series of numbers (Table 1, in appendix 1) between the current dry decade (since 1997) and the driest decade on record (1936 to 1945), three reasons for this “*amplification*” were proposed:

- (1) About 60 per cent of the rainfall decline is concentrated in autumn (67 per cent in the five month period from March to July); this precedes the period (winter/spring) typically associated with the largest runoff during the year. During the previous dry decade the autumn decline was less than one third of the total rainfall decline.
- (2) The year to year variability (measured by the standard deviation in each period) has been lower during this decade than the previous dry decade. This result, underlining the absence

of any year markedly in excess of the long-term average, is likely to have exacerbated the impact on river systems and reservoirs.

- (3) The on-going warming is likely to have increased the evaporation and reduced the amount of water available for run-off. The current decade occurred with maximum day-time temperatures about 0.7 °C higher. This is a very significant warming (about 1.5 times the standard deviation over the long-term means).

The focus on autumn is somewhat misleading and a better understanding of the regional pattern of the decline across SEA is captured by projecting on the annual cycle of the total rainfall. In the southern part of SEA, most of the rainfall occurs during the cold months from the autumn break to spring. There the largest decline (in absolute term) is in late autumn to early winter as rainfall in early autumn is negligible. On the contrary, in the northern part of SEA where more rainfall falls during the warmer month, the decline is most noticeable in summer to autumn (C. Rakich and P. Wiles, personal communication). A convenient way to separate between the two regions is to use the location of the STR. The STR has a marked annual cycle; during autumn it varies rapidly between a mean summer position of 38 °S and a mean winter location of 31 °S and sits around 35 °S (Drosowsky, 2005). We have used the position and intensity of the STR as calculated by Drosowsky (2005): a meridional profile of MSLP is averaged using monthly MSLP values between 147.5 and 152.5 °E and interpolated to a fine 0.5° latitudinal resolution using cubic spline, the absolute maximum pressure of this profile is assumed to be the position of the STR.

Also as part of Project 1.1.1, the current state of the science regarding the climate of SEA was reviewed (Murphy and Timbal, 2007) and preliminary analyses of the importance of several large-scale modes of variability were conducted (Timbal and Murphy, 2007). It showed that in that particular time of the year, there is very little influence from remote large-scale modes of variability on the local rainfall whereas most of the rainfall decline could be related directly to regional MSLP trends.

All the findings listed above and coming from the first project of the SEACI were used to help focus this project. Rainfall trends were studied separately between the south-west of eastern Australia (SWEA) and a large area on the other side of the STR. The focus on autumn was tuned to early winter in SWEA and warm season rainfall further north. Amongst the large-scale mode of variability, only the role of the SAM was investigated further as it appears that the strength of the teleconnections between tropical SSTs in both the Pacific (linked to ENSO) and the Indian Ocean (linked to IOD) and the rainfall in SEA is relatively weak overall. These relationships tend to vary with time and in the case of the SWEA have been declining in the last 20 years (Timbal et al., 2008b). This finding suggests that the rainfall decline in most of the SEA (at least in the southern winter-rainfall dominated area) is unlikely to be explained by the time-evolution of these tropical modes of variability as, if anything, their influence on the local rainfall is rather small and diminishing in last the two decades. It was also noted that in the SWEA the on-going rainfall trend is consistent with future projections (Timbal and Jones, 2008).

Past trends in the Southern Annular Mode and their role on rainfall and MSLP

The Southern Annular Mode (SAM) describes a naturally occurring oscillation of pressure between the mid-latitudes of the southern hemisphere and the southern polar region. The high-phase of SAM is characterised by higher than normal pressure over the southern mid-latitudes and lower than normal pressure over Antarctica. Conversely, the low-phase of SAM is characterised by lower than normal pressure over the mid-latitudes and higher than normal pressures over the pole.

The importance of the Southern Annular Mode (SAM) on Australian temperature and rainfall has been documented (Hendon et al., 2007). Subsequently, the same analysis was redone across the SEACI domain using high resolution gridded rainfall (Fig. 1 in appendix 2). It reveals that rainfall on and south of the Great Dividing Range across Victoria is more related to SAM than previously thought. This could be an important result as this mountainous area is a high rainfall area and is important to generate run-off for most of the Eastern part of Victoria. Comparison of the monthly and seasonal interactions shows that the SAM-rainfall relationship is much more robust on seasonal timescales. Month to month relations are less statistically reliable due to the small number of days in each phase and do not confirm a possible role in SAM to explain the month to month variability in rainfall decline: large in April, May and July but not in June (Murphy and Timbal, 2007).

The seasonal relationship calculated by Hendon et al. (2007) was adapted to match the key seasons for SWEA: early winter (May–June–July), where observed rainfall has declined and SAM index is trending upward, and late winter (August–September–October), where rainfall has not declined and SAM is not trending upward. It was found that a rainfall decline of 5 per cent in MJJ could be attributed to the SAM trend using the Marshall (2003) SAM index from 1959 onward (this is well below the observed decline in this region of about 11 per cent at this time of the year (Timbal et al., 2008a). In ASO, there is hardly any rainfall decline attributable to SAM (below 1 per cent) since the index has hardly any trend since 1959. Taken at face value, these estimates indicate that almost 50 per cent of the total decline in rainfall could be attributable to the SAM increase. However closer inspection of the timing of SAM changes, and rainfall changes, indicate that the relationship is perhaps more complex. While the SAM increased during the 1960s and 1970s, the rainfall decline has occurred only since the mid-1990s.

The work of Hendon et al. (2007) was adapted for MSLP. It shows that, for all seasons, increasing SAM is associated with increasing pressure above SEA, with the largest signal in the observations occurring in MJJ. Using the Marshall SAM index, the observed trend on SAM index can be translated into a MSLP rise of 0.5 hPa in the vicinity of SEA. This is a significant amount up to one third of the observed MSLP increase in MJJ. Even higher number were obtained using NCEP based SAM index but the result in this case are more doubtful as the NCEP SMA index is questionable prior to 1979. As for rainfall, there is a timing issue as most of the MSLP increase above the eastern part of Australia has happen since the 1970s (Timbal et al., 2008a).

Future trends in the SAM and their role on rainfall and MSLP

Climate models are very consistent in predicting that global warming will lead to a more permanent high-phase of the Southern Annular Mode. Models are also very consistent in projecting a winter-time rainfall reduction affecting southern Australia, including the SWEA. Hendon et al. (2007) analysis was adapted and applied to a series of climate simulations with the CSIRO Mk3.5 global climate model: a 2000-year long control simulation (i.e. no external forcings such as greenhouse gas increases) used to obtain statistical significance of the results under 'natural' climate variability, a simulation of the 20th Century with all known external natural and anthropogenic forcings and a projection for the 21st Century forced with anthropogenic forcings according to the SRES A2 emission scenario.

Figure 2 in the appendix provides a global perspective for the contribution of SAM to rainfall in the Southern Hemisphere from the CSIRO model. This is the pattern of rainfall changes one would expect from an increasingly positive SAM index. The model appears to perform very well since the results are consistent with the observations across Australia, in particular the rainfall reductions in the south-east of the continent, as well as the south west. This change is most likely associated with increases in local pressure, and a southerly shift in the storm systems that bring wintertime rainfall to these regions.

Trends in the SAM are analysed for various 30-year periods from all CSIRO simulations and compared to the observations (Table 2). In order for all the SAM indices to be comparable we used a MSLP based index as it is the case with the Marshall index. This is because surface pressure is a variable that is more easily obtainable from climate model simulations. The SAM index estimated from NCEP reanalysis of surface pressure shows larger positive changes in winter and spring than the Marshall index. In comparison the CSIRO model underestimates the observed trends during the 20th Century. The future projected trends for the 21st Century are very comparable to the modelled trends for the 20th Century.

Then the model SAM signal is translated into a rainfall signal using Hendon et al. (2007) to project SAM related rainfall and pressure changes in a future, warmer world and to compare these estimates to the total rainfall and pressure projections in the future climate scenario. The rainfall changes for the south-east of the continent expected from future changes in SAM using the CSIRO model are quite sizeable for both 30-year periods: 2031–2060 and 2061–2090 relative to pre-industrial climate (Table 3.1). The underlying SAM-rainfall relationship for south-eastern Australia is calculated from the model by considering multiple 30-year samples from the 2000-year control simulation. Similarly uncertainty in the underlying SAM-rainfall relationship is calculated from the distribution of 30-year samples. The SAM related rainfall change accounts for around 60 per cent (2031-2060) and 30 per cent (2061-2090) of the total predicted trend in MJJ rainfall in the CSIRO climate change projections.

Similarly, the SAM-pressure signal accounts for between 60 per cent and 95 per cent of future MJJ and JJA pressure changes (Table 3.2). For the periods 2031–2060 and 2061–2090, for autumn and winter months, the SAM related changes in pressure account for a much higher proportion of total pressure changes in the CSIRO climate projections when compared to rainfall. A caveat to this result is that SAM related changes account for much more of the total pressure changes in the model compared to the observed for the 20th Century.

In general, the SAM-pressure correlations are more robust than those for rainfall. This result perhaps reflects the fact that rainfall has a much higher level of variability or climate noise compared with pressure. In particular the signal to noise ratio of the SAM-pressure relationship in the long control simulation is much higher than that for the SAM-rainfall relationship. Changes in pressure associated with SAM may therefore be a more robust way to characterise future SAM related climate change for southern Australia.

It is planned to continue this analysis by applying it to a selection of IPCC-AR4 climate models in order to compare with these results based on the CSIRO model and investigate the consistency amongst models of this triangular relationship: SAM index, MSLP and rainfall above the SEA.

The role of the sub-tropical ridge on south-east Australian rainfall

The role of the STR on SWEA revealed that up to 80 per cent of the MJJ rainfall decline could be related to the strengthening of the ridge since the 1970s (Timbal et al., 2008b). It is worth noting that the timing of the increase of the STR intensity corresponds better to the rainfall decline than the SAM related rainfall decline mentioned earlier (in the 1960s and 1970s). Furthermore, during that earlier period the STR intensity was relatively low compared to the previous dry decades of the 1940s and 1950s and that might have compensate the expected SAM related decline.

We have extended the analysis of the role of STR across the entire SEA region and across the months for which the rainfall decline is largest: from March to July. Across SEA, rainfall in March–April–May–June–July has decreased from a mean of 262 mm.year⁻¹ from 1950 to 1980 to a mean of 201 mm.year⁻¹ since 1997 (a 23 per cent decline). The MAMJJ decline represents 57 per cent of the total decline (note that percentage is lower than when the reference period is 1961-1990 as shown on page 3). Although, the relationship between MSLP and rainfall is strongest in winter, it remains significant in autumn and overall quite high over the entire MAMJJ period (Table 4). Correlations with the STR intensity are higher than with direct MSLP and in MAMJJ explain up to 35 per cent of the inter-annual variability (Fig. 3).

The long-term evolution of the intensity of the STR in MAMJJ was compared to the average surface temperature of the globe (data from the Climatic Research Unit, University of East Anglia, UK). For both variables, 21-year running annual means were calculated (Fig. 4) centred on the 20th Century (to have a mean of zero on the graph) and using different Y-axes (on the left for the STR and on the right for global temperature). The long-term co-evolution of both variables is remarkable. The previous high values of the STR correspond to the 1940s to 1950s when the global temperature reaches a maximum before decreasing until the 1960s and then rising again after the 1970s as does the global temperature. Using the slope of the relationship (-31.5 mm.hPa⁻¹) it is possible to translate the intensification of the STR from the low values between 1950 and 1980 to the record high since 1997 into a rainfall signal equivalent to 43mm.year⁻¹. This amounts to 70 per cent of the observed decline. This amount is comparable, albeit lower than the similar role of the STR for the MJJ rainfall decline in SWEA where the same calculation indicated that up to 80 per cent of the observed decline could be linked to the STR intensification (Timbal et al., 2008b). It shows that although, the role of STR intensification is

strongest in the south-west of the SEACI domain, where winter rainfall dominates it can be felt across the entire domain.

North of the sub-tropical ridge: the role of MSLP gradient on rainfall

In addition to diagnosing the role of the STR on rainfall and of the role of the SAM, south of the STR, a further analysis has been conducted on the relationship between rainfall in the northern part of the SEA and large-scale forcing using a newly developed MSLP index: the Gayndah-Deniliquin Index or GDI (Rakich et al., 2008). This index represents the variability in the trade wind flow over eastern Australia bringing moisture inland from the surrounding Tasman Sea and relates particularly well with warm season (summer and autumn) rainfall (correlation of 0.76) in NSW (Fig. 5). This index exhibits large decadal variability corresponding to abrupt changes in rainfall over vast areas of the eastern Australian continent where warm season rainfall dominates.

An analysis of the relative contributions of each pole of the index (Fig. 6) reveals that until 1946, the MSLP variations at the two locations were roughly synchronized, leading to a relatively stable GDI. In contrast, during the late 1940s and early 1950s, a strong rise in Deniliquin MSLP combined with a fall in MSLP at Gayndah resulted in a rapid rise in the GDI at the time when most of SEA started to experience its wettest 30-year period on record. Since the 1970s, MSLP at the northern pole (Gayndah) has been rising, slowly regaining levels seen prior to 1947. The recent sharp decline in the GDI has resulted from this continued rise of summer MSLP at Gayndah, combined with a sudden decline of summer MSLP at Deniliquin since 2000 at a time where the protracted drought which was already well underway in SWEA started to extend to the rest of eastern Australia

The GDI was found to be complementary to the ENSO in summer and autumn, when the south-easterly trade winds affect eastern Australia and the SOI-rainfall relationship is at its weakest. Of interest, it was found that the relationship between the GDI and the SOI was asymmetric as is the ENSO-rainfall relationship: an asymmetry between positive and negative phases (see Power et al., 2006 in the case of ENSO) which as a consequence generates a inter-decadal variability of the strength of the relationship during El Niño dominated and La Niña dominated epochs (see Power et al., 1999 in the case of ENSO). Similarly the GDI-rainfall exhibits multi-decadal variability in the strength of the relationship. That suggests that although complimentary, the relationship between the GDI and warm season rainfall over eastern Australia is not independent of ENSO.

Can the heat wave of April 2005 be attributed to global warming?

It is usually acknowledged that it is difficult to attribute a single extreme event to climate change; on the other hand, it is possible, if the frequency of particular extreme events is observed to increase, to attempt to attribute such increases. In the case of hot temperature and heat waves, a number of records have been established in the last decade or so and there has been some attempt to attribute this increase to on-going global warming. In this study, we have decided to investigate a single extreme event (rather than the frequency of occurrence) with

large and severe impacts: the heat waves of April 2005. On a national scale, April 2005 saw the most extreme temperature anomalies ever recorded for Australia (NCC, 2005). The Australian mean temperature was 2.58 °C above the 1961–90 average, nearly 1 °C above the previous April record (1.73 °C in 2002), and well above the largest anomaly previously recorded for any month (2.32 °C in June 1996). Averaged across the Murray–Darling Basin (MDB), the anomaly was spectacular: 4 °C (almost 1.5 °C above the previous record in 2002).

The Bureau of Meteorology Statistical Downscaling Model (SDM) has been used to examine the role of day-to-day meteorological conditions in producing the extreme temperatures across the MDB. The large-scale MSLP and temperature at 850 hPa (T_{850}) have been used to see whether the heat waves can be explained by natural variability in the atmospheric circulation or whether global warming is a major contributor. The model takes analogues from a “pool” of MSLP and/or T_{850} fields from 1958–2004 to reproduce the situation in April 2005.

First the ability of the SDM to reproduce the observed temperature inter-annual variability and trend over the entire 1958 to 2004 period was evaluated. The T_{850} predictor was able to reproduce much of the year-to-year variations in stations surface maximum temperatures and had more skill than the MSLP predictor. This skill generally improved when the two predictors were used together. It was found that changes in MSLP patterns in April should have resulted in cooling temperature trend at MDB stations, whereas the T_{850} patterns produced no trend when averaged across MDB stations. However, combining both large-scale circulation and temperature produces a positive, but weaker than observed, temperature trend. This result is difficult to interpret; it suggests that part of the surface temperature trend across the basin can be accounted for by changes in synoptic situations combined with warmer air aloft, thus emphasising the importance of mid-tropospheric warming to explain the surface trends. However, the absence of trend when MSLP is used as a single predictor clearly demonstrates that the on-going warming across the basin cannot be explained by changes in synoptic situations.

Then the SDM was applied in a cross-validated mode to try to reproduce the heat wave of April 2005. The T_{850} patterns reproduce about half of the observed hot anomaly in April 2005 across the MDB while MSLP reproduces very weak and generally negative anomalies (Figure 7). When the two predictors are combined, the anomalies are in most cases smaller. The results show that the April 2005 heat wave cannot be accounted for by anomalous synoptic situation (i.e. it was not due to a series of anomalous meteorological situations). On the contrary the warming of the troposphere appears critical and explains about half of observed surface heat wave.

Acknowledgement: This work was funded by the South Eastern Australia Climate Initiative.

Outputs from this project

Publications:

- (1) Hendon, H.H., D.W.J. Thompson, and M.C. Wheeler, 2007: Australian rainfall and surface temperature variations associated with the Southern Annular Mode. *Journal of Climate*, **20**, 2452-2467
- (2) Rakich, C., N. Holbrook and B. Timbal, 2008: A pressure gradient metric capturing planetary-scale influences on eastern Australian rainfall. *Geophysical Research Letters*, **35**, L08713, doi:10.1029/2007GL03297
- (3) Timbal, B. and D. Jones, 2008: Future projections of winter rainfall in southeast Australia using a statistical downscaling technique. *Climatic Change*, **86**, 165-187.
- (4) Timbal, B., Hope, P. and R. Fawcett, 2008: On the relationship between rainfall in the southwest and the southeast of Australia. Part I: Variability on daily and longer time-scales, *Journal of Climate*, submitted
- (5) Timbal, B., Wheeler, M. and P. Hope, 2008: On the relationship between rainfall in the southwest and the southeast of Australia. Part II: Possible causes of recent declines, *Journal of Climate*, submitted

Conference papers:

- (1) B. Murphy., B. Timbal and D. Jones, 2007: "A Tool for Attribution of Climate Anomalies", *Australian Meteorological and Oceanographic Society 14th National Conference*, Adelaide, February 2007.
- (2) B. Timbal and P. Hope, 2006: "On the relationship between South West and South East Australian winter rainfall", *17th Australian New-Zealand Climate Forum*, Canberra, September 2006.
- (3) B. Timbal. 2007: "Winter rainfall in Southern Australia: Past and future trends", *International Union of Geodesy and Geophysics General Assembly*, Perugia, Italy, July 2007.
- (4) B. Timbal. 2007: "Observed climate changes in the south-east of Australia: detection and possible attribution", *Hydrological consequences of climate change*, Canberra, November 2007.

References

- Drosowsky, W., 2005: The latitude of the subtropical ridge over eastern Australia: the L index revisited. *International Journal of Climatology*, **25**, 1291-1299
- Hendon, H.H., D.W.J. Thompson, and M.C. Wheeler, 2007: Australian rainfall and surface temperature variations associated with the Southern Annular Mode. *Journal of Climate*, **20**, 2452-2467
- National Climate Centre, 2005: An exceptionally warm April and dry start to 2005. *Special Climate Statement*, **5**, April 2005
- Murphy, B.F. and B. Timbal, 2007: A review of recent climate variability and climate change in south eastern Australia. *International Journal of Climatology*, DOI: 10.1002/joc.1627
- Power, S., F. Tseitkin, V. Mehta, B. Lavery, S. Torook, and N. Holbrook, 1999: Decadal climate variability in Australia during the twentieth century, *International Journal of Climatology*, **19**, 169-184
- Power, S., M. Haylock, R. Colman, and X. Wang, 2006: The predictability of interdecadal changes in ENSO activity and ENSO teleconnections, *Journal of Climate*, **19**, 4755-4771
- Rakich, C., N. Holbrook and B. Timbal, 2008: A pressure gradient metric capturing planetary-scale influences on eastern Australian rainfall. *Geophysical Research Letters*, **35**, L08713, doi:10.1029/2007GL03297
- Timbal, B., Hope, P. and R. Fawcett, 2008a: On the relationship between rainfall in the southwest and the southeast of Australia. Part I: Variability on daily and longer time-scales, *Journal of Climate*, submitted
- Timbal, B., Wheeler, M. and P. Hope, 2008b: On the relationship between rainfall in the southwest and the southeast of Australia. Part II: Possible causes of recent declines, *Journal of Climate*, submitted
- Timbal, B. and D. Jones, 2008: Future projections of winter rainfall in southeast Australia using a statistical downscaling technique. *Climatic Change*, **86**, 165-187
- Timbal, B. and B.F. Murphy, 2007: Observed climate change in South-East of Australia and its relation to large-scale modes of variability. *BMRC Research Letter*, **6**, 6-11

Appendix: 1: Tables

Table 1: Mean and standard deviation for total rainfall, autumn (March–April–May) rainfall, annual temperature and Murray River modelled inflow for three period: 1997–2006, 1936–1945 and 1961–1990.

Period vs. Variables	1997-2006		1936-1945		1961-1990	
	Mean	Std	Mean	Std	Mean	Std
Total Rain (mm)	511	90	494	106	595	120
Autumn Rain (mm)	98	32	116	36	149	51
Tmax (°C)	20.4	0.27	19.7	0.47	19.9	0.48
Murray Inflow (GL)	4872	2722	5855	4406	9437	5541

Table 2: Trend in SAM expressed as units of standard deviation from Observations and for future climate model projections. The trends are expressed as 30-year trends using 11-year low pass filtered data. Projections indicate a tendency toward a high-phase in the months May through to August.

Season	Observed 1971-2006	CSIRO GCM 1971-2000	CSIRO GCM 2001-2030
DJF	0.81	0.61	-0.11
MAM	1.92	-0.06	0.13
MJJ	1.71	0.41	0.79
JJA	1.51	0.74	1.03
SON	0.20	0.22	0.00

Table 3.1: Future projected changes in rainfall (mm) due to changes in the Southern Annular Mode under global warming (SRESA2) emissions scenario. The GCM SAM-Forced rainfall amounts represent the implied change in rainfall due to future SAM.

	2031-2060		2061-2090	
	SAM-Forced Rainfall Trend	per cent of total projected rainfall trend	SAM-Forced Rainfall Trend	per cent of total projected rainfall trend
DJF	0.91	-4.39	0.89	-3.35
MAM	2.15	-21.89	2.36	-12.12
MJJ	-7.47	62.67	-9.45	30.89
JJA	-6.43	38.28	-9.25	28.61
ASO	0.06	-1.16	0.21	-0.62
SON	1.17	-51.99	3.17	-10.23

Table 3.2: Future projected changes in pressure (hPa) due to changes in the Southern Annular Mode under global warming (SRESA2) emissions scenario. The GCM SAM-Forced rainfall amounts represent the implied change in rainfall due to future SAM.

	2031-2060		2061-2090	
	SAM-Forced Pressure Trend	per cent of total projected Pressure trend	SAM-Forced Pressure Trend	per cent of total projected Pressure trend
DJF	4.48	31.97	4.38	-10.69
MAM	40.26	71.90	44.21	42.51
MJJ	115.00	68.86	145.55	65.27
JJA	96.00	94.12	138.00	91.39
ASO	19.42	-176.51	64.22	91.74
SON	15.48	110.55	41.88	62.51

Table 4: Pearson correlation between MSLP or the intensity of the sub-tropical ridge (STR-I) and the rainfall averaged across the SEA region for several period: autumn (March to May), March to July and early winter (May to July). The bold correlation is used to infer a rainfall reduction linked to the STR intensification across SEA.

	SEA rainfall		
	MAM	MAMJJ	MJJ
MSLP	-0.29	-0.53	-0.68
STR-I	-0.42	-0.59	-0.70

Appendix: 2: Figures

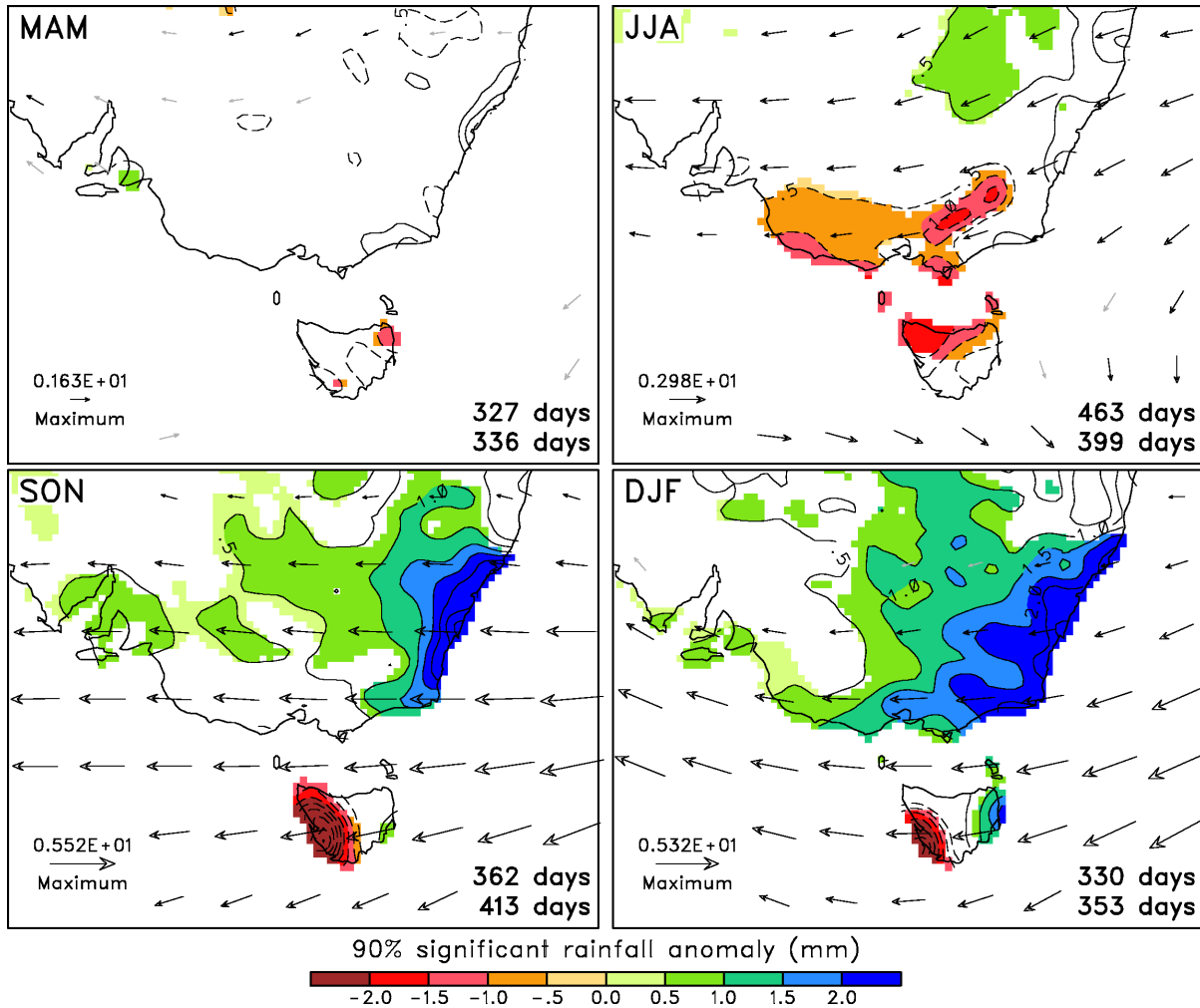


Figure 1: Composite daily rainfall (contours and shading) and 850 hPa winds (maximum vector shown in lower left corner of each panel) for high minus low polarity of the SAM index for MAM (top left), JJA (top right), SON (bottom left) and DJF (bottom right), using daily data (1979 to 2005). Significant differences at the 90 per cent level are shaded. The number of days in the high and low index polarity of the SAM is listed in each panel.

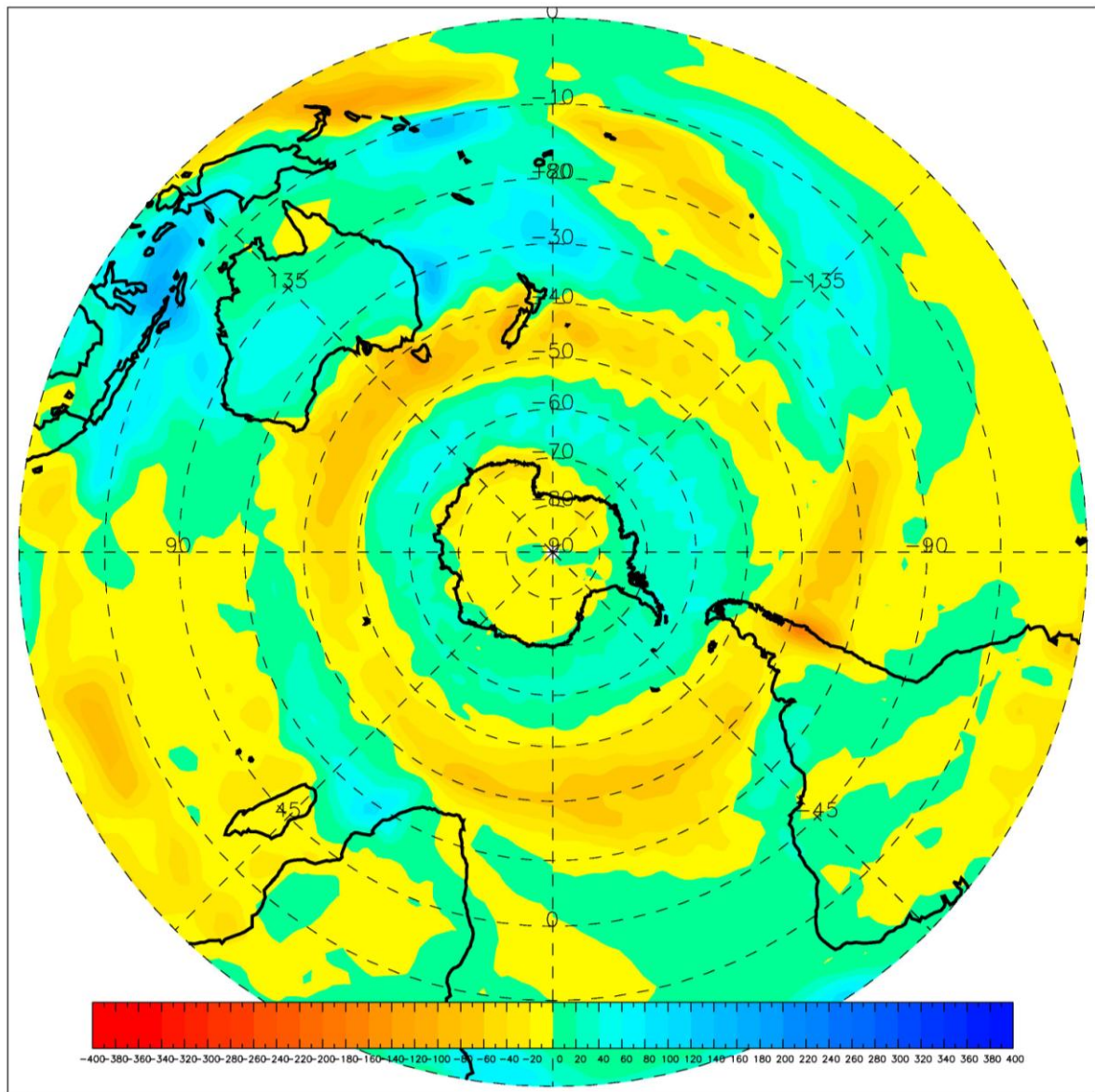


Figure 2: Mean Composite Rainfall difference for seasonal (MJJ) SAM high-low phase events. Negative values indicate a net rainfall reduction for that region associated with high-phase SAM. South west Western Australia and south eastern Australia are regions associated with reduced rainfall during high phase SAM.

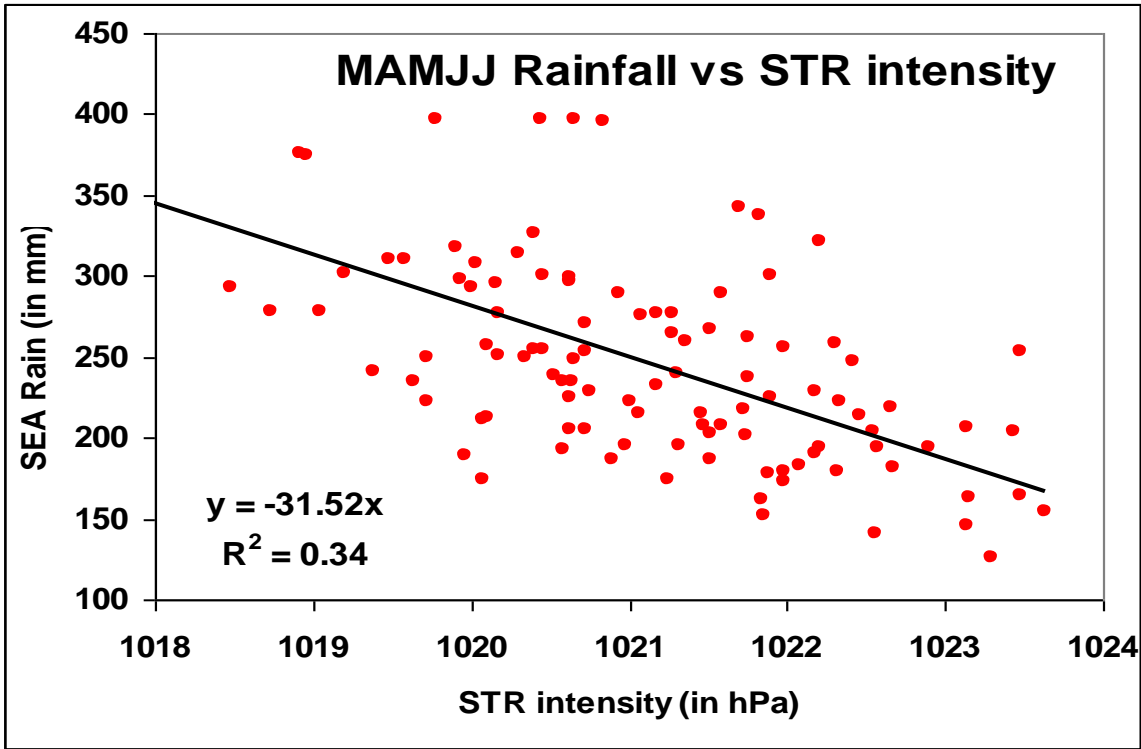


Figure 3: Relationship between SEA March-April-May-June-July rainfall and the sub-tropical ridge (STR) intensity during the same five months. The slope of the linear relationship and the amount of explained variance (r^2) is shown in the lower left corner.

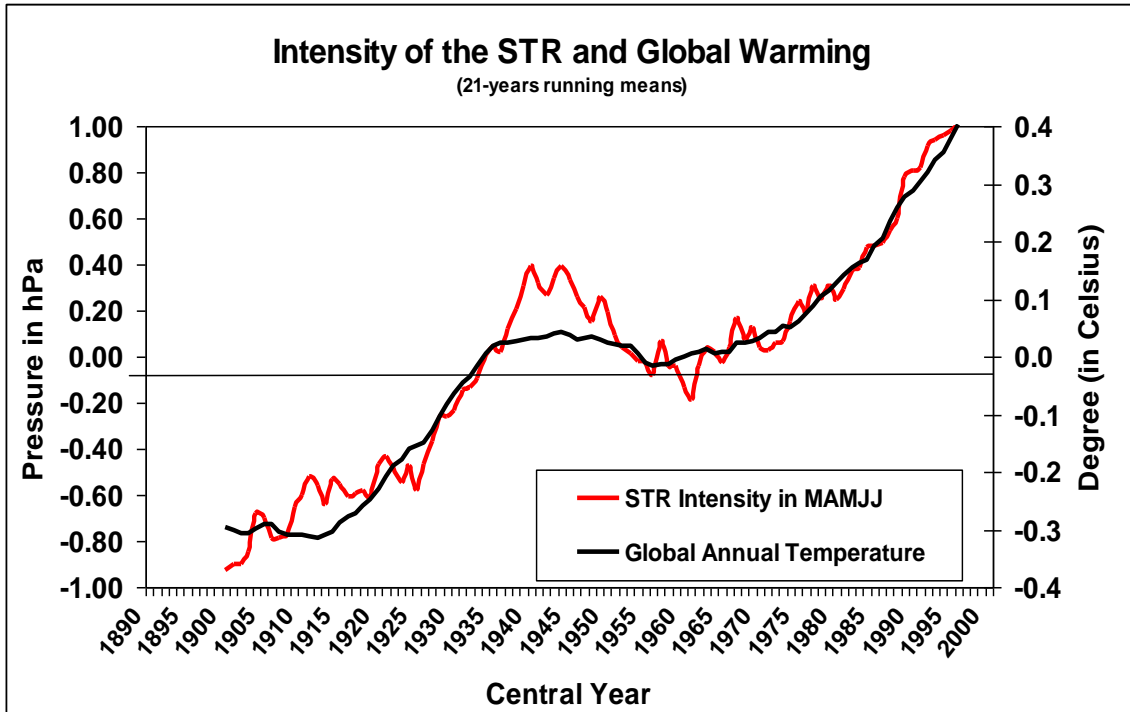


Figure 4: Long-term (21-year running mean) evolution of the sub-tropical ridge (STR) March-April-May-June-July mean intensity (anomalies in hPa shown on the left-hand Y-axis) compared with the global annual surface temperature (data are from the Climate Research Unit in the UK; anomalies were calculated as per the STR curve and are in Degree Celsius shown on the right-hand Y-axis).

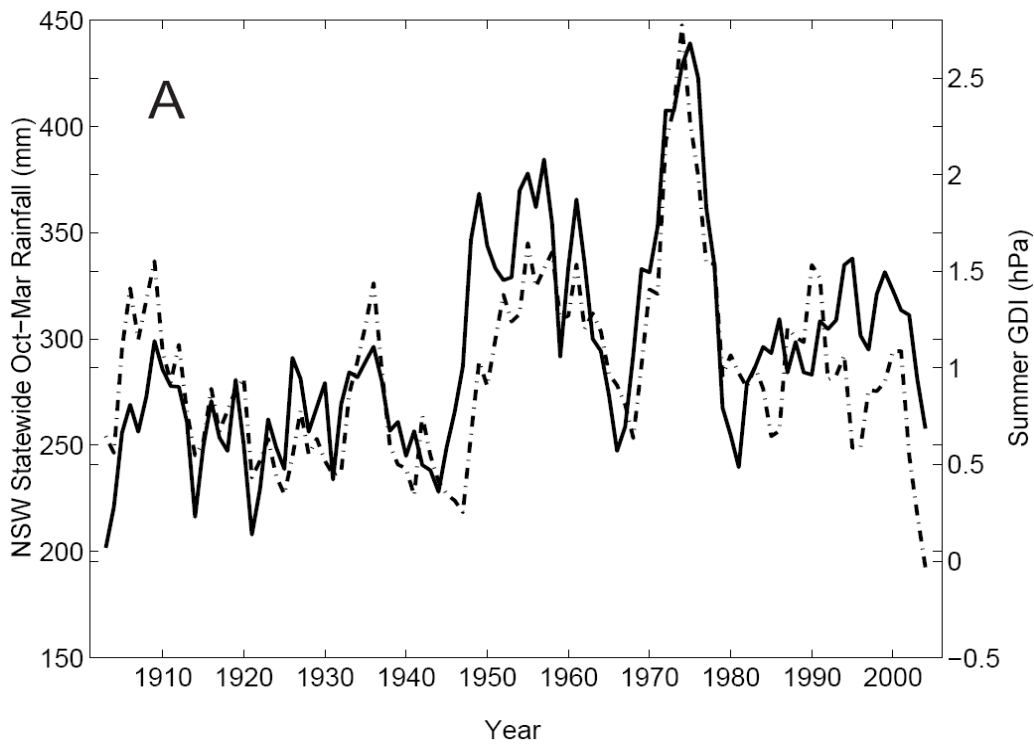


Figure 5: Five-year moving averages of both the warm season (Oct-Mar) NSW state-wide average rainfall (solid line) and the summer GDI (dashed line).

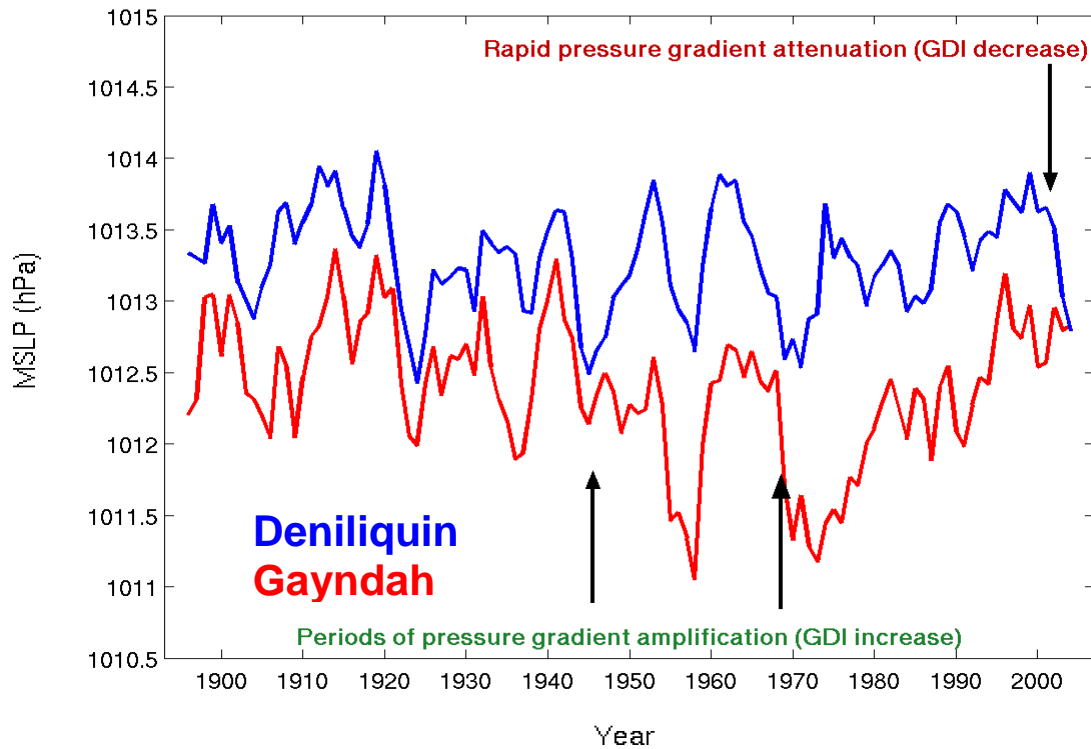


Figure 6: Five-year moving averages of summer (DJF) MSLP at Gayndah, QLD (red line) and Deniliquin, NSW (blue line) showing periods of rapid pressure gradient amplification (e.g. late 1940s and late 1960s) and rapid pressure gradient attenuation (e.g. mid 1960s and 2000–2006).

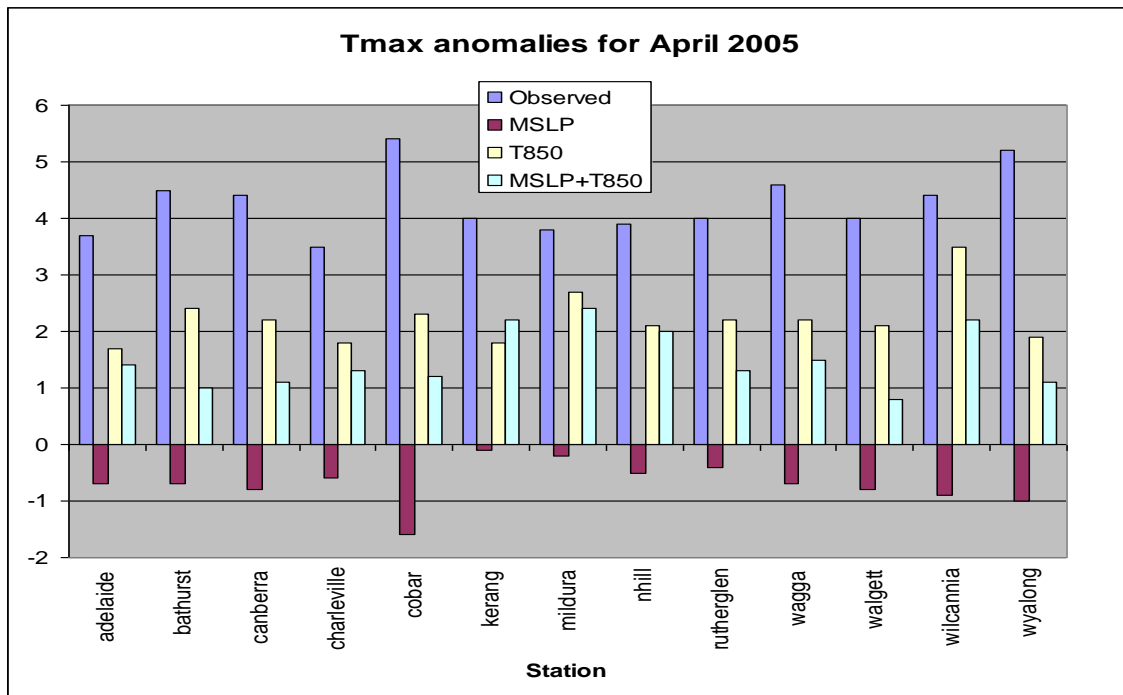


Figure 7: Mean maximum temperature anomalies for April 2005 observed and as simulated by downscaling model with MSLP, T_{850} and MSLP/ T_{850} as predictors.